Eq. (2)

$$\bar{L} = \begin{bmatrix} \bar{\eta}^T\bar{a} - \bar{V}^T\bar{V} \\ \bar{R}^T\bar{V} \\ 0 \end{bmatrix} \quad (16)$$

where $\bar{a}$ is the acceleration at the terminal time τ. For this guidance law,

$$G_1 = G_2K^{-1}H,\ G_2 = [\bar{c}\bar{c}^T/\bar{c}^T\bar{c}] - I \quad (17)$$

and the vector $\bar{c}$ is defined by

$$\bar{c} = K^{-1}\bar{L} \quad (18)$$

The constraints represented by Eqs. (10–12) also may be used to construct a VTA guidance law which computes $\delta\tau$ to minimize the distance from the nominal target point.[7]

Results and Discussion

The reference trajectory chosen to illustrate the guidance laws outlined in the preceding sections is a 1977 Mars-orbital mission discussed in considerable detail in Ref. 9. The maneuver required to target the spacecraft to the entry corridor is assumed to be executed at the Earth sphere of influence (SOI). The assumed imperfect execution of this maneuver necessitates the subsequent midcourse maneuvers, which are the subject of this Note. The position and velocity uncertainties at the time of this maneuver are 300 naut miles and 1 fps; the corresponding dispersions are 900 naut miles and 8 fps. The nominal entry conditions are an altitude h_E of 400,000 ft and flight path angle γ_E of $-6°$, which result in an entry speed V_E of 38,250 fps. The time required for the spacecraft to reach the Earth-entry interface from the Earth SOI is 64 hr. The inclination of the entry trajectory i_E is 75°.

The root-mean-square (rms) entry radius, speed, and flight path angle dispersions are presented in Fig. 1 as a function of the rms midcourse ΔV. The midcourse maneuever execution errors are assumed to be a 1% proportional error, a 1° pointing error, and a $\frac{1}{2}$-fps engine cut-off error.[4] Earth based radar measurements were assumed to be made once per hour.

In Fig. 1a, the FTA guidance law is formulated to null position vector errors at the nominal time of arrival at the entry interface. This figure is indicative of an optimum time to execute the midcourse maneuver and produce minimum values of the entry parameter dispersions for the smallest propellant expenditure. However, the optimum time for minimum dispersion is different for each of the entry parameters. The techniques discussed in Ref. 10 could be used to determine analytically the optimum single correction times, but such a determination is beyond the scope of this Note.

In Fig. 1b, the FTA guidance law is formulated to null radial, cross-range, and γ_E errors at the nominal time of arrival at the entry interface. As might be expected, the γ_E control is better for this guidance law.

The dispersions for the VTA guidance laws are presented in Figs. 1c–1e. The entry-speed errors are generally lower than the corresponding errors for the FTA guidance laws, but these differences are misleading, because, for the VTA guidance laws, an associated plot of the rms timing error (data not shown) maps into a velocity error, and this velocity error, in effect, must be added to the speed error computed from the VTA guidance equations. For the VTA guidance laws considered typical timing errors are 150–300 sec. However, the relaxation of the constraint on the time of arrival permits a smaller rms ΔV requirement for specified radius and γ_E errors. For the trajectory considered (which is representative of a conjunction-class Mars mission), the best over-all performance is produced by the guidance law which is formulated to null radial, cross-range, and γ_E errors while the magnitude of the commanded ΔV is minimized (Fig. 1d).

References

[1] Battin, R. H., *Astronautical Guidance*, McGraw-Hill, New York, 1964.

[2] Stern, R. G., "Interplanetary Midcourse Guidance Analysis," Vol. 1, CR-51827, 1964, NASA.

[3] White, J. S., Callas, G. P., and Cicolani, L. S., "Application of Statistical Filter Theory to the Interplanetary Navigation and Guidance Problem," TN D-2697, 1965, NASA.

[4] Murtagh, T. B., Lowes, F. B., and Bond, V. R., "Navigation and Guidance Analysis of a Mars Probe Launched from a Manned Flyby Spacecraft," TN D-4512, 1968, NASA.

[5] Robbins, H. M., "An Analytical Study of the Impulsive Approximation," *AIAA Journal*, Vol. 4, No. 8, Aug. 1966, pp. 1417–1423.

[6] Cicolani, L. S., "Linear Theory of Impulsive Velocity Corrections for Space Mission Guidance," TN D-3365, 1966, NASA.

[7] Tempelman, W., "Linearized Impulsive Guidance Laws," *AIAA Journal*, Vol. 3, No. 11, Nov. 1965, pp. 2148–2149.

[8] Ribarich, J. J. and Meredith, C. M., "Analysis of Surveyor Midcourse Guidance as a Problem in the Theory of Maxima and Minima," *Journal of Spacecraft and Rockets*, Vol. 3, No. 7, July 1966, pp. 997–1001.

[9] Lowes, F. B. and Murtagh, T. B., "Navigation and Guidance Systems Performance for Three Typical Manned Interplanetary Missions," TN D-4629, 1968, NASA.

[10] Murtagh, T. B., "Optimum Interplanetary Midcourse Velocity-Correction Schedules," *Proceedings of the Fourth Congress of the International Federation of Automatic Control*, Warsaw, Poland, 1969, pp. 19–38; also *The IFAC Journal, Automatica*, Pergamon Press, New York, Vol. 6, No. 1, Jan. 1970, pp. 99–109.

Low-Thrust Mission Simulation–Feedback to Hardware Definition

ALFRED C. MASCY*

NASA Ames Research Center, Moffett Field, Calif.

AMONG the major functional elements of solar and nuclear electric propulsion mission simulation are the representation of the high- and low-thrust planetocentric and heliocentric trajectories, and the necessary definition of the powerplant, thruster, and power-conditioning characteristics. There is always interplay between the elements, and each has its unique role in the over-all optimization criteria. Mission analyses should provide feedback to the hardware developers, and vice versa. Feedback effects for two levels of sophistication are indicated in Fig. 1. A computer program along these lines is presently being developed.[1] This Note briefly describes the approach and presents some examples of the influences of powerplant and thruster characteristics for unmanned Saturn orbiter missions.

Returning to Fig. 1, high- and low-thrust trajectory optimization may be accomplished by rapid, level 1 type routines or by higher precision, level 2 type routines. Level 1 modules use functional relationships for the energy requirements of precomputed optimum trajectories obtained from accurate computer programs.[2] Curve-fitting procedures have been employed to define the energy parameter, J, as a function of time and hyperbolic excess velocity V_∞ at Earth departure and planet arrival. A method of system optimization, based on the invariance of J with system parameters, was found to be quite accurate.[3] Low-thrust planetocentric operations are expressed analytically, em-

Presented at the AIAA 7th Electric Propulsion Conference, Williamsburg, Va., March 3–5, 1969 (no paper number; published in bound volume of conference papers); submitted April 28, 1969; revision received February 18, 1970.

* Research Scientist, Mission Analysis Division, Office of Advanced Research and Technology. Member AIAA.

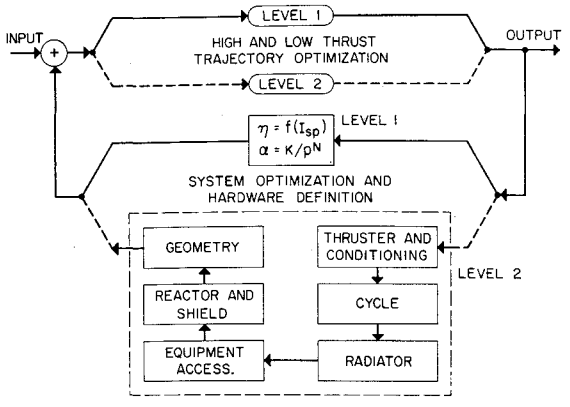

Fig. 1 Flow chart of computer program showing feedback and levels of sophistication.

ploying the method of Breakwell-Rauch for asymptotic matching of the planetocentric-heliocentric phases.[4] High-thrust stages may be used for departure or arrival at a planet, and the performance characteristics of launch vehicles are built-in so that missions may be simulated from the ground up.[5] The interplay between high- and low-thrust systems is considered in the optimization of V_∞. Correlation with exact trajectory data is excellent, and the computer times are much less than 1 sec per optimized case. If more refined simulation is required, the code may be operated in a level 2 mode which will recompute the mission using a detailed trajectory subroutine with the level 1 parameters as an initial starting solution. The execution times for this scheme are greatly reduced, since in the lower level of analyses the trajectory data have already been computed, and in the higher level, excellent initial solutions are available for the optimization of system and trajectory parameters such as specific impulse, powerplant mass fraction, thrust acceleration, operating time, and V_∞ at departure and arrival.

In level 1, the functional relationship of system parameters, such as powerplant specific mass (α), thruster efficiency, and operating time, are included in the code. After a broad spectrum of missions has been examined and narrowed to a reasonable number by use of level 1 type hardware description, the code may then be used in level 2, within which the system is detailed into subsystem modules, including thruster and power conditioning mating, thermodynamic cycle calculations, radiator weight and area analysis, apportionment of accessory equipment, pumps, plumbing, etc., reactor characteristics, shield weight breakdown, and geometric configuration design and weight summary. There are, of course, feedback loops and optimizations between the various subsystems, which may be subject to mission constraints such as distance from sun, ambient temperature, operating time, power level, diameter of launch vehicle, etc. Level 1 of hardware definition is built-in to an operational code and individual subsystem subroutines[6] of level 2 are presently in check-out status. When fully developed, the level 2 mathematical modeling of the powerplant characteristics will allow the interplay necessary to an overall low-thrust mission simulation tool.

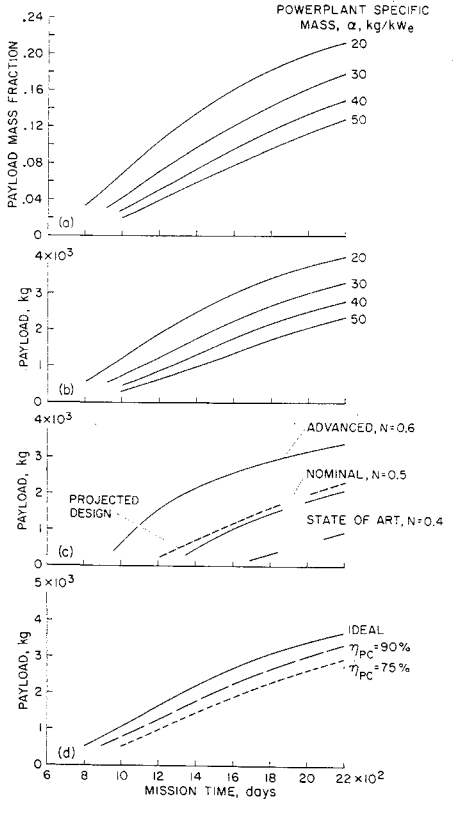

Fig. 2 Payload vs mission time for Saturn orbiters: a) parametric effect of α for launch from low Earth orbit; b) absolute payload using Titan III F/Centaur, from ground; c) dependence on powerplant technology (where $\alpha = 350/P^N$; and d) dependence on thruster efficiency.

Some Effects of Powerplant and Thruster Characteristics

An unmanned probe is assumed to be placed in a circular orbit about Saturn at a distance of 20 Saturn radii. Figure 2a shows the effect of mission time on payload mass fraction (the fraction of initial mass in a low Earth circular parking orbit delivered to the orbit about Saturn) for various α's. This type of parametric analysis is warranted when a large number of cases are to be examined and when gross comparisons are to be made with other systems, modes, or missions.[7] These data were obtained assuming departure from a 185-km-altitude, circular orbit with a chemical stage having a specific impulse of 450 sec. If the launch system chosen has an upper stage of approximately the same characteristics, then these results can be used to determine absolute payloads.

In Fig. 2b, the absolute performance for the same Saturn orbiter mission is presented using a particular launch vehicle, the Titan III F/Centaur. However, the mission is now assumed to start from the ground up, and the launch system is used to provide a hyperbolic boost away from Earth. The burnout velocity of the launch system has been optimized along with the low-thrust system in order to maximize absolute payload. These results relate to a unique launch vehicle and define the maximum performance of the combined high- and low-thrust systems. The power level has been optimized at each point along the curves and varies widely, particularly for the lower powerplant specific masses (α's). This variation in the optimum power level along a payload-triptime curve does not allow a natural selection of a best-suited powerplant size for the launch vehicle and mission under consideration.

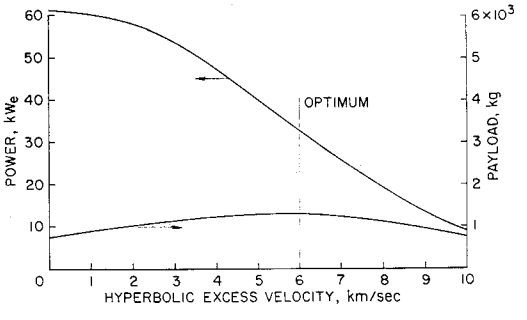

Fig. 3 Trade-off between launch vehicle capability and operating power level—Titan III F/Centaur launch system.

The range of uncertainty in α is too large to identify a reasonable compromise power level.

To delineate the influence of powerplant characteristics on mission performance, various technology levels were assumed for a nuclear power-plant such that $\alpha = 350/P^N$ kg/kw_e, where P is power in kw_e. Exponents (N's) of 0.6, 0.5, and 0.4 were assumed to represent advanced, nominal, and state-of-the-art technology levels, respectively. The state-of-the-art technology estimates a 30-kw_e plant to weigh about 90 kg/kw_e while a larger 300-kw_e plant would weigh about 35 kg/kw_e. The "nominal" estimate ($N = 0.5$) shows a 30-kw_e plant to have an α of 64 kg/kw_e while the 300-kw_e plant would weigh about 20 kg/kw_e. (Any such estimates require periodic updating and improvement by those cognizant in the development of such hardware, of course.) The solid curves in Fig. 2c represent these assumed technology levels for the same Saturn orbiter mission. Each point on one of these solid curves represents a completely optimized mission, including a powerplant which has been optimally sized for the particular mission and the Titan III F/Centaur launch vehicle. Accordingly, the optimum power level varies slightly along each curve. For $N = 0.5$, it is near 50 kw_e and varies no more than 5% from this value. For any one mission, the launch system has the major influence on power level. When the most appropriate P for the launch vehicle mission parameters has evolved, the case may be analyzed using this fixed P with a fixed weight representative of a technology level. The dotted curve in Fig. 2c represents a 50-kw_e, 2500-kg powerplant, which is near the optimum in the "nominal technology" case.

The selection of a compromise power level for a particular launch vehicle does not seriously affect mission payloads. In Fig. 3, the power and payload for a 1600-day Saturn mission are shown relative to the V_∞ provided by the Titan III F/Centaur launch system during Earth departure. The optimum power for this mission would be 33 kw_e, requiring a V_∞ of 6 km/sec. However, the power level employed may be 50% larger or smaller than the optimum and yet the payload decreases only about 15%, since the launch system is used to make up much of the deficiency by providing less or more V_∞, respectively. This type of "off-optimum" operation will almost certainly exist when more than one mission, mission mode, or trip time is considered. For this particular example, a nuclear powerplant was examined. Solar-cell powerplants would have similar trade-off characteristics. In addition, a further trade-off which includes the cost per kilowatt of power may influence the "compromised" selection.

Another major functional element of both solar and nuclear electric systems is the over all efficiency η_{ts} of the thruster subsystem, including the power conditioning. Depending on the type of thruster and power conditioning, the projected over all efficiency may vary widely. In Fig. 4, estimates[8,9] of mid-1970 η_{ts}'s for mercury electron-bombardment thrusters are shown which assume power conditioning efficiencies (η_{PC}'s) of 90% and 75%. The missions examined thus far have assumed the thruster subsystem efficiency curve having an η_{PC} equal to 90%. The effects of η_{ts} on the performance for the Saturn orbiter mission, for which the specific impulse ranges from 4000 to 7000 sec as time increases, are shown in Fig. 2d. Obviously, η_{PC} and η_{ts} must be assessed accurately,

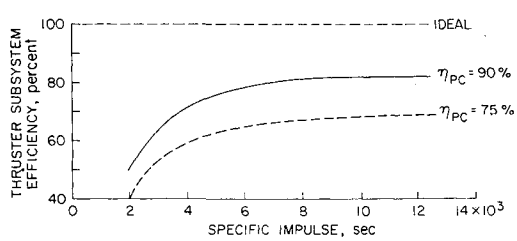

Fig. 4 Thruster subsystem efficiency.

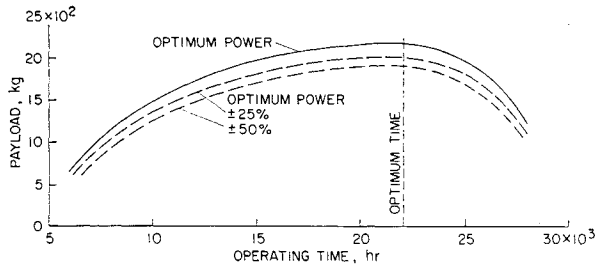

Fig. 5 Effect of thrusting time on performance for 1600-day, Saturn orbiter mission.

particularly for difficult missions or for spacecraft with heavy powerplants.

Thruster or powerplant operating lifetime may also enter the mission-system analysis interplay. For near-term solar-electric systems, available thrusters may be limited in operating time; for nuclear-electric systems, powerplant lifetime may also be a constraint. Figure 5 shows the effect of thrusting time on net spacecraft mass, or payload, for an example 1600-day Saturn orbiter mission. The optimum thrusting time is 22,000 hr. A decrease to 15,000 hr causes a decrease of ~10% in payload; a further reduction to 11,000 hr causes the payload to decrease by ~30%. Increases in thrust operating time beyond the optimum value appear to be more costly in performance. This would be the case if there were no reactor or solar-cell shutdown permitted, and, instead of coasting, propellant was consumed unnecessarily. Off-optimum power levels appear to have the same payload-operating time trade-off characteristics. The performance of systems whose power level is 25% (or 50%) less or greater than the optimum power level is shown by the dashed curves.

Concluding Remarks

Meaningful mission analyses must include feedback through hardware definition. Examples presented herein have indicated that, through the relationship between powerplant specific mass and power level, a power-plant size can be selected which will accommodate many missions. The launch vehicle has a predominant influence on this selection. However, launch vehicle capability can be traded off with power level to lessen the loss in performance due to off-optimum sizing of the powerplant. Thruster efficiency also plays a strong role in the over-all optimization, and there should be emphasis on its system definition and its mission implications. Thruster or powerplant operating time constraints should be considered in the over-all mission-system analysis interplay.

Several degrees of sophistication in mission analysis-hardware feedback loops are possible through the combination of computer program modules of increasing complexity, many of which are already available. The modeling of subsystem characteristics requires continual updating through the mutual exchange of information between the mission analyst and the hardware developer.

References

[1] Mascy, A. C., "A Computer Program for Quickly Analyzing Electric Propulsion Missions," Working paper MP 69-4, Aug. 22, 1969, Mission Analysis Div., OART/NASA.

[2] "Study of Trajectories and Upper Stage Propulsion Requirements for Exploration of the Solar System," NASA Contract NAS2-2928, Final Report, July 15, 1966, United Aircraft Research Labs., East Hartford, Conn.

[3] Melbourne, W. G. and Sauer, C. G., Jr., "Payload Optimization for Power-Limited Vehicles," TR 32-250, April 1962, Jet Propulsion Lab., California Institute of Technology, Pasadena, Calif.

[4] Breakwell, J. V. and Rauch, H. E., "Asymptotic Matching in Power-Limited Interplanetary Transfers," paper 66-114, 1966, American Astronautical Society.

[5] Mascy, A. C., "Extraecliptic 1.0 a.u. Constant Power Electric Propulsion Missions," *Journal of Spacecraft and Rockets*, Vol. 6, No. 12, Dec. 1969, pp. 1367–1371.

[6] Mascy, A. C., "A Compilation of Current Computer Programs for Low-Thrust Trajectory and Mass Computation," TM X-1824, July 1968, Mission Analysis Div., OART/NASA.

[7] Mascy, A. C., Dugan, D. W., and Pitts, S. W., "Applications of Combined High-Thrust, Low-Thrust Propulsion Systems," *Journal of Spacecraft and Rockets*, Vol. 5, No. 7, July 1968, pp. 785–791.

[8] Masek, T. D. and Pawlik, E. V., "Thrust System Technology for Solar Electric Propulsion," *Journal of Spacecraft and Rockets*, Vol. 6, No. 5, May 1969, pp. 557–564.

[9] Richley, E. A. and Kersloke, W. R., "Bombardment Thruster Investigations at the Lewis Research Center," *Journal of Spacecraft and Rockets*, Vol. 6, No. 3, March 1969, pp. 289–295.

Pressure Measurements and Gas-Flow Analysis in Chambers A and B during Thermal-Vacuum Tests of Spacecraft 2TV-1 and LTA-8

H. K. F. EHLERS*
NASA Manned Spacecraft Center, Houston, Texas

UNLIKE the actual situation in space, a vehicle in a space simulation chamber is directly exposed to areas that reflect molecules coming from the vehicle and even areas that emit molecules, e.g., cables, pipes, support structures, and other ground support equipment (GSE). Moreover, the test objectives may require the release of large quantities of liquids and gases (such as water, glycol, O_2, N_2, H_2 etc.) from vents of the spacecraft, thus increasing the flow of reflected molecules. At the NASA Manned Spacecraft Center in 1968, a study was made of the pressures and the gas flows in various locations and directions, both in Chamber B which housed the Apollo Lunar Module, LTA-8, and in Chamber A which housed the Apollo Command and Service Module, 2TV-1, during testing that involved these requirements. This Note outlines the determination of specific test-article or chamber conditions by identifying and locating gas sources inside the vacuum chambers during the thermal-vacuum tests and by evaluating the effect of the gases on the simulation of space vacuum. Additional information on the space simulation chambers is available from the literature.[1,2]

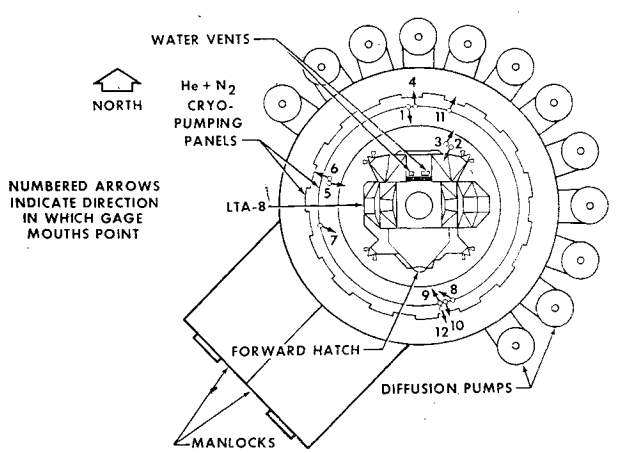

Fig. 1 Ion-gage locations 1–12 in Chamber B for LTA-8. (Chamber B has inside dimensions of 25 ft diam × 30 ft height.)

Presented as Paper 69-1033 at the AIAA/ASTM/IES 4th Space Simulation Conference, Los Angeles, Calif., September 8–10, 1969; submitted September 25, 1969; revision received November 24, 1969.

* Head, Research and Development Section.

Analysis and Gage Features

For simplicity, the spacecraft and the "chamber surface" are represented in the math model by concentric spheres, and it is assumed that the outer sphere has a cryopumping capability equal to the total effective pumping capability of the simulation chamber pumping systems. The capture coefficient (s_c) of the chamber surface (assuming homogeneous spherical distribution) is the fraction of gas molecules pumped during one encounter. By placing pairs of ion gages (with one gage pointing at the test-article surface (inner sphere) and the other gage pointing at the chamber surface) near the surface of the test article or near the chamber surface, one can determine the total directional gas flows and the gas load emitted by the test-article. However, the gages cannot distinguish between reflected and emitted molecules. To determine s_c, the gas emittance of the outer sphere must be known. For good simulation, the degassing and leak rates of the chamber and GSE must be small compared with the degassing and leak rates of the test article. Because gages mounted near the spacecraft usually interfere with spacecraft activities and other test objectives, the use of gages near the chamber surface is preferable.

Let us define[3] Z as the ratio of the number of molecules returning to vehicle surface to the number of molecules initiating at vehicle surface. Then

$$Z = AX/(Y - X) \tag{1}$$

where Y is the gas-flux density at a gage located near the chamber surface and directed toward the test article; X is the gas-flux density at a gage located near the chamber surface and directed toward the chamber surface; and A is the probability that a molecule leaving the chamber surface will strike the vehicle. A low value for Z is desired. It is

$$X/Y \approx 1 - s_c \tag{2}$$

in a good space simulation chamber. Also, it is important to note that s_c varies with the type of gas in the chamber. The relatively high pumping speed of liquid nitrogen (LN_2) panels for gases and vapors which condense at LN_2 temperatures, "condensibles," must be distinguished from the relatively low pumping speed for gases which do not condense at LN_2 temperatures, "noncondensibles." Table 1 gives typical values of Z and X/Y based on estimates of s_c and calculated from Eqs. (1) and (2) (A = 0.3 and 0.06 respectively).

The s_c's and Z's for the condensibles are good, and the corresponding X/Y ratios are sufficiently small to permit determination of the directional gas flow when ion gages with normal calibration error are used for the measurements. The higher values for the noncondensible gases, indicating quasi-

Table 1 Z, X/Y, and s_c; calculated data

	Chamber A (2TV-1)		Chamber B (LTA-8)	
	Noncondensibles[a]	LN_2 cold walls	Noncondensibles[a]	LN_2 cold walls
s_c	0.08	0.95	0.1	0.95
Z	0.7	0.003	2.7	0.015
X/Y	0.92	0.05	0.9	0.05

[a] Pumped by helium cryopumps and diffusion pumps.